Journal of Organic and Pharmaceutical Chemistry

Original Research

OPEN ACCESS
Freely available online on
http://ophcj.nuph.edu.ua

UDC [547.792.9+547.789.69]:615.31

N. I. Korol[1], V. V. Pantyo[1], V. O. Bestritska[1], K. A. Avdeeva[1],
D. I. Molnar-Babilya[2,3], M. M. Fizer[4], M. V. Slivka[1]

[1] Uzhhorod National University, 53/1 Fedytca Str., 88000 Uzhhorod, Ukraine
[2] Ferenc Rákóczi II Transcarpathian Hungarian Institute, 6 Kossuth Sq., Beregovo 90200, Ukraine
[3] Mukachevo State University, 26 Uzhhorodska Str., 89608 Mukachevo, Ukraine
[4] University of Nevada Reno, 1664 N. Virginia Str., 89557 Reno, NV, United States

Antimicrobial and Antifungal Study of Thiazolotriazolium Salts: *in vivo* Investigation, and Molecular Docking

Abstract

Three thiazolo[3,2-*b*][1,2,4]triazol-7-ium hexabromotellurates **1**–**3** were synthesized *via* the electrophilic heterocyclization of methallyl thioether precursors using a classical tellurium(IV) electrophilic reagent generated *in situ* from TeO_2 and 1 M hydrobromic acid. The resulting salts were comprehensively screened for the antimicrobial activity against five clinically relevant pathogens: *Staphylococcus aureus*, *Candida albicans*, *Klebsiella pneumoniae*, *Escherichia coli*, and *Pseudomonas aeruginosa*. Biological assays revealed that compound **1** containing a 2-(4-pyridyl) substituent demonstrated the strongest activity profile, particularly against *C. albicans* (MIC = 15.625 μg mL^{-1}) and *E. coli* (MIC = 31.25 μg mL^{-1}). Compound **2**, substituted with the 3-hydroxyphenyl moiety, also showed a significant antifungal efficacy, while compound **3** (with the 2-phenyl substituent) exhibited a relatively low activity. To rationalize these differences, the molecular docking was performed targeting MurB (UDP-N-acetylenolpyruvoylglucosamine reductase, PDB 1MBT) and DNA gyrase B (GyrB, PDB 4URO), two bacterial enzymes known to be essential for the viability of Gram-negative pathogens. The docking results confirmed the experimental data, showing strong π–π stacking and hydrogen bonding between compound **1** and the FAD-containing binding pocket of MurB. This work highlights the utility of the tellurium-induced annulation in producing biologically potent heterocycles and emphasizes the structure–activity relationships driven by substituents in position 2 of the fused scaffold.

Keywords: [1,3]thiazolo[3,2-*b*][1,2,4]triazol-7-ium hexabromotellurates; anti-microbial activity; docking; electrophilic cyclization; MurB; GyrB; molecular docking

Н. І. Король[1], В. В. Пантьо[1], В. О. Бестріцька[1], К. А. Авдєєва[1], Д. І. Молнар[2,3], М. М. Фізер[4], М. В. Сливка[1]

[1] Ужгородський національний університет, вул. Фединця, 53/1, м. Ужгород, 88000, Україна
[2] Ференца Ракоці ІІ Закарпатський Угорський Інститут, пл. Кошута, 6, м. Берегово, 90200, Україна
[3] Мукачівський державний університет, вул. Ужгородська, 26, м. Мукачево, 89608, Україна
[4] Університет Невади (Рено),
вул. Н. Вірджінія, 1664, м. Рено, 89557, Штат Невада, Сполучені Штати Америки

Антимікробне й протигрибкове дослідження солей тіазолотриазолію: *in vivo* вивчення та молекулярний докінг

Анотація

Три тіазоло[3,2-*b*][1,2,4]триазол-7-ій гексабромтелурати **1**–**3** синтезовано електрофільною гетероциклізацією металіл-тіоетерів з використанням класичного електрофільного реагенту на основі телуру(IV), отриманого *in situ* з TeO_2 та 1 М бромоводневої кислоти. Отримані солі ретельно досліджено на антимікробну активність проти п'яти клінічних штамів: *Staphylococcus aureus, Candida albicans, Klebsiella pneumoniae, Escherichia coli* та *Pseudomonas aeruginosa*. Мікробіологічними дослідженнями виявлено, що сполука **1**, яка містить 2-(4-піридил)-замісник, продемонструвала найсильніший профіль активності, особливо проти *C. albicans* (МІК = 15.625 мкг $мл^{-1}$) та *E. coli* (МІК = 31.25 мкг $мл^{-1}$). Сполука **2**, заміщена 3-гідроксифенільним фрагментом, також продемонструвала значну протигрибкову ефективність, тоді як сполука **3** (з 2-фенільним замісником) продемонструвала порівняно низьку активність. Щоб раціоналізувати ці відмінності, було проведено молекулярний докінг на ферментах MurB (UDP-N-ацетиленолпірувоїлглюкозамін редуктаза, PDB 1MBT) та ДНК-гірази B (GyrB, PDB 4URO), які відіграють важливу роль у життєдіяльності грамнегативних бактерій. Результати докінгу підтвердили експериментальні дані, показавши сильний π–π-стекінг та водневі зв'язки між сполукою **1** та кишенею зв'язування MurB, що містить FAD. Ця робота підкреслює корисність індукованої телуром

ISSN 2308-8303 (Print) / 2518-1548 (Online)

ануляції для отримання біологічно активних гетероциклів та акцентує на взаємозв'язках структура-активність, зумовлених замісниками в положенні 2 конденсованого каркаса.

Ключові слова: [1,3]тіазоло[3,2-*b*][1,2,4]триазол-7-ій гексабромтелурати; антимікробна активність; докінг; електрофільна циклізація; MurB; GyrB; молекулярний докінг

Citation: Korol, N. I.; Pantyo, V. V.; Bestritska, V. O.; Avdeeva, K. A.; Molnar-Babilya, D. I.; Fizer, M. M.; Slivka, M. V. The Antimicrobial and Antifungal Study of Thiazolotriazolium Salts: *in vivo* Investigation, and Molecular Docking. *Journal of Organic and Pharmaceutical Chemistry* **2025**, *23* (4), 44–56.

https://doi.org/10.24959/ophcj.25.344433

Received: *3 October 2025*; **Revised:** *17 November 2025*; **Accepted:** *25 November 2025*

Funding: The research was carried out with the grant support of the National Research Foundation of Ukraine (project No 2023.03/0176).

Conflict of interests: The authors have no conflict of interests to declare.

■ Introduction

The escalating global health threat posed by the antimicrobial resistance (AMR) across bacterial and fungal pathogens necessitates continuous, intensive efforts to identify structurally novel antimicrobial agents [1–3]. The emergence of multidrug-resistant (MDR) organisms has rendered many conventional antibiotics ineffective, leading to the increased morbidity and mortality worldwide. Consequently, modern medicinal chemistry prioritizes the development of new compounds with unique scaffolds that can circumvent resistance mechanisms [4, 5].

Among the most promising classes of molecules are heterocyclic compounds containing fused nitrogen- and sulfur-containing rings. These scaffolds exhibit a notable conformational rigidity, redox properties, and binding specificity, positioning them as privileged frameworks for the drug design [6–16]. Specifically, thiazole-fused systems, such as thiazolotriazoles, have attracted attention due to their broad spectrum of biological activities, including antimicrobial, antiviral, antioxidant, and enzyme-inhibitory effects [13, 17–23]. Their aromatic rigidity and electron-rich structure enable fine-tuning of pharmacodynamic and pharmacokinetic parameters.

A powerful synthetic approach for assembling such heterocycles involves electrophilic heterocyclization [24]. In particular, reactions mediated by tellurium(IV) electrophiles (generated *in situ* from TeO_2 and aqueous hydrobromic acid) have enabled the efficient introduction of the tellurium moiety into condensed heterocyclic salts with the pharmaceutical potential [25–27]. Tellurium-containing organic compounds have the biological potency [28–32], but their behavior in biological systems has not been elucidated to date [33]. As previously reported in our works, the electrophilic heterocyclization method provides access to bioactive thiazolotriazole $TeHal_3$ frameworks

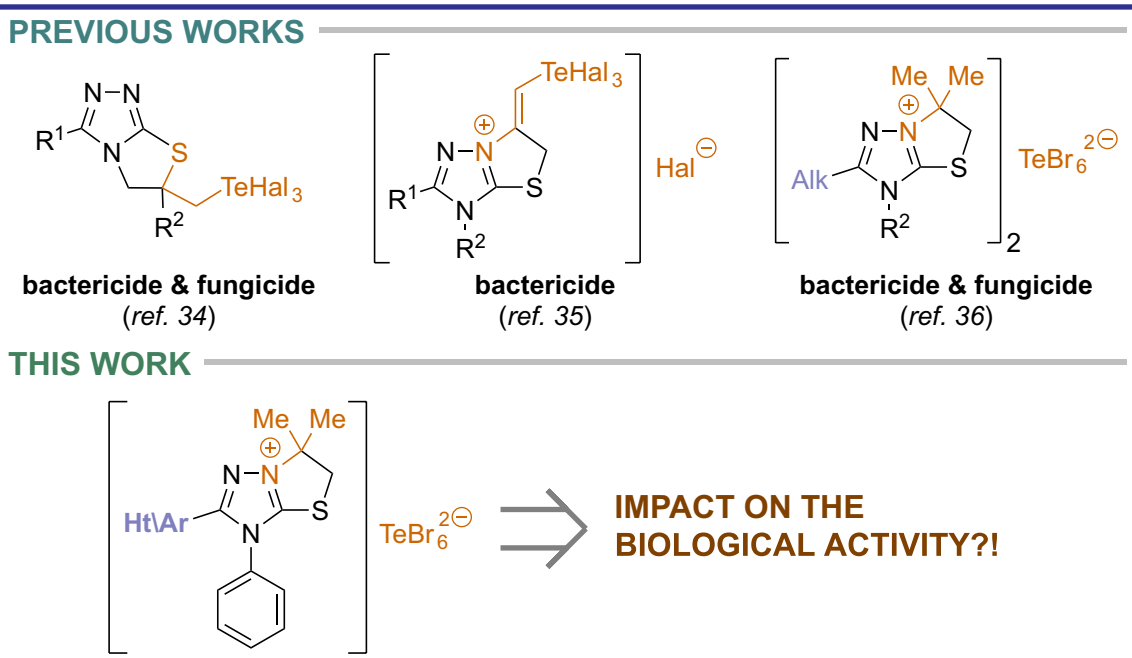

Figure 1. The synthesis of bioactive thiazolotriazole derivatives

in excellent yields under mild conditions [34, 35] (**Figure 1**). An additional design element involves incorporating the halotellurate anion, which can improve the bactericidal and fungicidal activity [36, 37]. This anion not only stabilizes the cationic framework, but also confers physicochemical properties that are beneficial for the biological activity, such as altered solubility, membrane permeability, and redox activity. Prior studies have shown that tellurium-based fragments can disrupt the microbial redox balance or form covalent bonds with intracellular thiols, thereby bypassing conventional resistance pathways [36].

Despite these promising features, the structure-activity relationship (SAR) studies for thiazolotriazolium salts remain underexplored. In particular, the effect of varying the substituent in position 2 of the heterocyclic core on the antimicrobial potency and selectivity is not well understood. To fill this gap, we synthesized and investigated three thiazolotriazolium hexabromotellurates with systematically varied position 2 substituents:

- Compound **1**: 2-(4-pyridyl), chosen for its capacity for the hydrogen bonding and the potential metal chelation.
- Compound **2**: 2-(3-hydroxyphenyl), to examine the role of the polar, hydrogen-bond-donating phenyl group.
- Compound **3**: 2-phenyl, serving as a neutral, lipophilic reference.

Following the synthesis, their antimicrobial activities were screened against representative Gram-positive (*Staphylococcus aureus*), Gram-negative (*Escherichia coli*, *Klebsiella pneumoniae*, *Pseudomonas aeruginosa*), and fungal (*Candida albicans*) strains. To rationalize the bioactivities observed, we conducted the predictive molecular docking against two bacterial enzymes: UDP-N-acetylenolpyruvoylglucosamine reductase (MurB, PDB ID: 1MBT), a key enzyme in the peptidoglycan biosynthesis, and DNA gyrase B (GyrB, PDB ID: 4URO), a crucial target for quinolone antibiotics [38]. These computational studies aimed to correlate the binding affinity and interaction profiles with experimental minimum inhibitory concentration (MIC) values and to identify structural determinants of activity.

Taken together, this study provides a comprehensive analysis of the antimicrobial potential of thiazolotriazolium hexabromotellurates and offers valuable insights into the SAR trends that govern their efficacy, supporting future optimization and development of this class of metallo-heterocyclic antibiotics.

■ Results and Discussion

Synthesis of compounds 1–3

The thiazolo[3,2-*b*]triazol-7-ium hexabromotellurate derivatives **1–3** were synthesized *via* a concise electrophilic heterocyclization of their respective methallyl thioether precursors (**Scheme 1**) similar to the procedure described [37]. This transformation was mediated by an *in situ*-generated tellurium(IV) electrophilic reagent, generated from tellurium dioxide (TeO_2) and hydrobromic acid in acetonitrile.

The above approach confers notable synthetic benefits as it simultaneously accomplishes the annulation of the fused heterocyclic core and the formation of the biologically active hexabromotellurate counterion $TeBr_6^{2-}$ in a single operational step. This dual-function transformation not only simplifies the workflow, but also enhances the atom economy and the isolation efficiency of the desired products **1–3**.

Antimicrobial and Antifungal Activity Evaluation

The antimicrobial and antifungal activities of compounds **1–3** were evaluated against *Staphylococcus aureus*, *Candida albicans*, *Klebsiella pneumoniae*, *Escherichia coli*, and *Pseudomonas aeruginosa* using MIC and MBC assays (**Table 1**). Specified strains were collected from the periodontal pockets of patients with chronic generalized

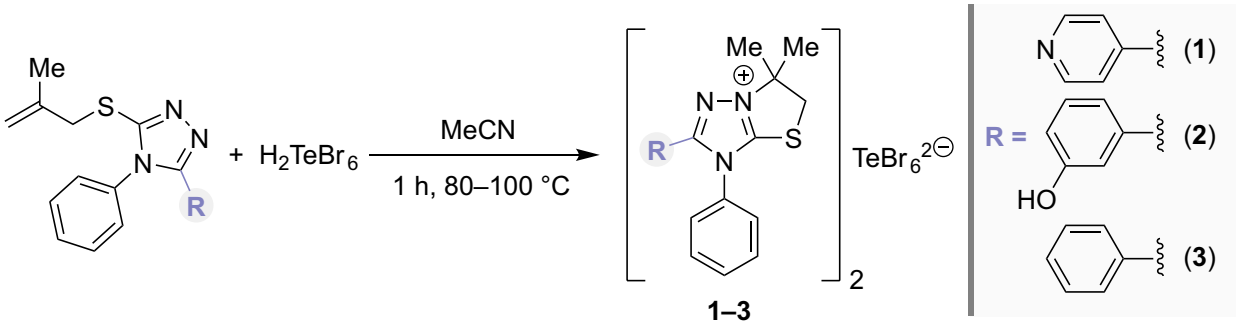

Scheme 1. The synthetic approach to [1,3]thiazolo[3,2-*b*][1,2,4]triazol-7-ium hexabromotellurates **1–3**

ISSN 2308-8303 (Print) / 2518-1548 (Online)

Table 1. The antimicrobial and antifungal activities of compounds **1–3** evaluated against *Staphylococcus aureus*, *Candida albicans*, *Klebsiella pneumoniae*, *Escherichia coli*, and *Pseudomonas aeruginosa* using MIC and MBC assays

Compound	Substituent	MIC / MBC, μg mL^{-1}				
		C. albicans	*S. aureus*	*K. pneumoniae*	*E. coli*	*P. aeruginosa*
1	4-pyridyl	15.625 / 62.5	125 / 250	125 / 125	31.25 / 62.5	125 / 125
2	3-hydroxyphenyl	15.625 / 31.25	62.5 / 250	125 / 125	125 / 125	125 / 250
3	phenyl	62.5 / 125	125 / 250	125 / 125	125 / 125	125 / 125
4[b]	methyl	31.25 / 125	31.25 / 62.5	7.81 / 15.63	1.95 / 3.9	– / –[a]
5[b]	heptyl	ND[a]	– / –[a]	1.95 / 15.63	62.5 / 125	250 / 500
6[b]	Pentadecyl	ND[a]	– / –[a]	31.25 / 62.5	15.63 / 31.25	62.5 / 125

Note: [a] "–" indicates that the compound was not active against the test organism at 500 μg mL^{-1}; ND – not determined; [b] compounds **4**, **5**, **6** were reported previously (**4** – compound **2a** [36]; **5** – compound **2b** [36]; **6** – compound 2d [36])

periodontitis who underwent treatment at the Uzhhorod University dental clinic. All three thiazolotriazolium salts demonstrated a measurable activity against this panel of clinically relevant pathogens, and were consistent with the well-established antimicrobial potential of thiazole- and triazole-based heterocycles [39–41].

To enrich the structure–activity relationship (SAR) analysis, the antimicrobial performance of compounds **1–3** was compared with that of previously reported 2-substituted thiazolotriazolium analogs from reference [36], specifically the aliphatic derivatives.

The MIC/MBC data reveal that the substituent in position 2 markedly influences the potency across both aromatic and aliphatic analogs. For the Gram-positive *S. aureus*, compound **2** (3-hydroxyphenyl) exhibited the lowest MIC (62.5 μg mL^{-1}) among compounds **1–3**. This potency is comparable to methyl derivative **4** (MIC ≈ 31.25 μg mL^{-1}), but superior to the bulky heptyl **5** and pentadecyl **6** (MIC > 500 μg mL^{-1}). All tested compounds **1–3** displayed primarily bacteriostatic effects, as evidenced by high MBC values (~250 μg mL^{-1}). Thus, while a polar aromatic substituent (compound **2**) or methyl group (**5**) improves MIC relative to the phenyl group or a bulky alkyl group, neither class substantially reduces the bactericidal concentration for this pathogen.

A different trend emerges with the fungal pathogen *C. albicans*. The aromatic derivatives **1** and **2** achieved a four-fold lower MIC (15.63 μg mL^{-1}) than the phenyl analog **3** and showed a stronger antifungal activity than the only aliphatic reference with available data (compound **4**, MIC ≈ 31.25 μg mL^{-1}). Antifungal data for the heptyl and pentadecyl derivatives (compounds **5** and **6**) were not determined (ND). These results indicate that polar and π-conjugated 2-substituents confer a superior antifungal potency, likely by facilitating stronger interactions with fungal targets or enhancing the membrane insertion, whereas very short or long alkyl groups are less favorable.

As MIC values are reported in μg mL^{-1}, equal mass concentrations do not always correspond to equal molar concentrations. When converted to micromoles per liter (μM), compounds **1** and **2** have nearly identical MIC values due to similar molecular weights, whereas among the aliphatic analogs, the heptyl derivative (compound **5**) has a higher molecular weight than the methyl derivative **4**, leading to the lower molar potency despite the identical MIC in μg mL^{-1}.

Against Gram-negative bacteria, distinct SAR profiles were observed. Compound **1** (4-pyridyl) was uniquely potent against *E. coli* (MIC 31.25 μg mL^{-1}), whereas compounds **2** and **3** required 125 μg mL^{-1} to inhibit the growth. None of the simple alkyl analogs from [36] matched this activity: even the heptyl derivative **5** inhibited *E. coli* only in 125 μg mL^{-1}. This underscores that the basic 4-pyridyl substituent that is capable of protonation and hydrogen bonding is far more effective in penetrating the Gram-negative outer membrane or engaging intracellular targets than hydrophobic groups. In contrast, all compounds displayed a modest activity against *K. pneumoniae* and *P. aeruginosa* (MIC ≥ 125 μg mL^{-1}). Even the long-chain **6** did not improve potency. It is consistent with the notion that excessive lipophilicity hinders penetration of Gram-negative envelopes. The heptyl analog **5** achieved sub-2 μg mL^{-1} MICs against certain *Klebsiella* isolates in [36], but lost its activity against Gram-positives, indicating a compromise, in which hydrophobicity favored Gram-negative uptake at the cost of Gram-positive efficacy. The small methyl substituent (**4**) maintained a broader, balanced profile.

Introducing polar functionality in position 2 markedly enhanced the activity against *C. albicans* and *S. aureus*. Compounds **1** (4-pyridyl) and **2** (3-hydroxyphenyl) both lowered the MIC four-fold relative to the unsubstituted phenyl

analog **3**, suggesting that hydrogen-bonding or dipolar groups were highly beneficial for the antifungal efficacy. The 4-pyridyl moiety introduces a basic nitrogen that can accept a proton and engage in the hydrogen bonding, while the 3-hydroxyphenyl group offers both donor and acceptor capability. These functionalities likely strengthen interactions with fungal biomolecules (e.g. enzymes or membrane components) and improve distribution in aqueous media. Compound **2** exhibited the lowest MBC against *C. albicans* (31.25 μg mL^{-1}), indicating a more rapid fungicidal effect when a hydroxyl group was present. On the contrary, the nonpolar phenyl group of compound **3** cannot enter into such interactions, correlating with its reduced potency.

Against *S. aureus*, only compound **2** showed a markedly improved MIC relative to other analogs, suggesting that a hydroxyl substituent is particularly advantageous for the Gram-positive activity. The simpler peptidoglycan-rich envelope of Gram-positive bacteria may allow easier penetration of polar compounds, and the hydrogen bonding likely enhances binding to targets. While compound **1** did not improve the MIC in *S. aureus* to the same extent, both polar-substituted derivatives (**1**, **2**) achieved lower MICs than the phenyl analog. Nonetheless, identical MBCs across the series imply that high concentrations remain necessary for the bactericidal activity against *S. aureus*.

E. coli was uniquely susceptible to compound **1**. Its MIC of 31.25 μg mL^{-1} is four times lower than that of compounds **2** or **3**. This selectivity arises from the properties of the 4-pyridyl substituent: the pyridine nitrogen can be protonated under physiological conditions, imparting a positive charge and the hydrogen-bonding capacity that may enhance interactions with the negatively charged lipopolysaccharide layer and facilitate passage through porins. Furthermore, compound **1** has a lower log*P* (~2.6) and a moderate polar surface area (~35 $Å^2$) relative to compounds **2** and **3** (log*P* ≈ 3.1 and TPSA ~42/22 $Å^2$), suggesting a more balanced polarity-lipophilicity profile suited to the Gram-negative penetration. By comparison, 3-hydroxyphenyl compound **2** carries a neutral polar group which higher TPSA may impede transit across the hydrophobic outer membrane; phenyl compound **3** is more hydrophobic and may be sequestered in membrane lipids or effluxed before reaching its target. These differences rationalize why only compound **1** exhibits a strong activity against *E. coli,* while the others do not. Against *K. pneumoniae* and *P. aeruginosa*, however, none of the 2-substituents were sufficient to overcome the formidable permeability barriers and efflux mechanisms characteristic of these species, resulting in uniformly modest MIC values.

Thus, the SAR trends reveal that the polarity and hydrogen-bonding capacity in position 2 dramatically improve the antifungal and Gram-positive activity, whereas an optimal balance of polarity and basicity (exemplified by the 4-pyridyl group) is crucial for the potent *E. coli* activity. Hydrophobic 2-substituents can enhance uptake in certain Gram-negatives (e.g., the heptyl group in **5** [36]), but tend to compromise the Gram-positive efficacy and do not outperform the polar analogs overall. In general, the new aromatic compounds **1–3** in almost all cases correspond to or exceed the activity of aliphatic analogs. In particular, the 4-pyridyl and 3-hydroxyphenyl substitutions increase the activity against *C. albicans*, *S. aureus,* and *E. coli* relative to simple alkyl groups, while an optimally sized alkyl chain (heptyl) offers the intermediate activity, but fails to rival the broad-spectrum efficacy of aromatic analogs. These findings highlight the value of incorporating the polar or π-conjugated functionality in C-2 to improve the antimicrobial profile of this scaffold.

***In silico* ADMET analysis of compounds 1–3**

To complement the experimental evaluation, we used ADMETlab to predict the absorption, distribution, metabolism, excretion, and toxicity profiles of compounds **1–3**. These models integrate physicochemical descriptors and machine-learning algorithms to estimate pharmacokinetic and safety parameters [42–45], offering a comparative view of how the three 2-substituents influence drug-likeness. A radar-plot visualizing the predicted physicochemical spaces of compounds **1–3** is presented in **Figure 2**.

As summarized in **Table 2**, all three cations tested fulfill Lipinski's rule-of-five criteria with molecular weights below 325 Da, log*P* values between ~2.6 and 3.2, and hydrogen-bond donor counts ≤ 1, indicating classical drug-like characteristics [46]. Compound **1** (4-pyridyl) exhibits the highest predicted aqueous solubility and unbound fraction, while compound **2** (3-hydroxyphenyl) has the largest topological polar surface area due to its phenolic OH and is predicted to be the least soluble. Compound **3** (phenyl) is the least polar and slightly more hydrophobic than

ISSN 2308-8303 (Print) / 2518-1548 (Online)

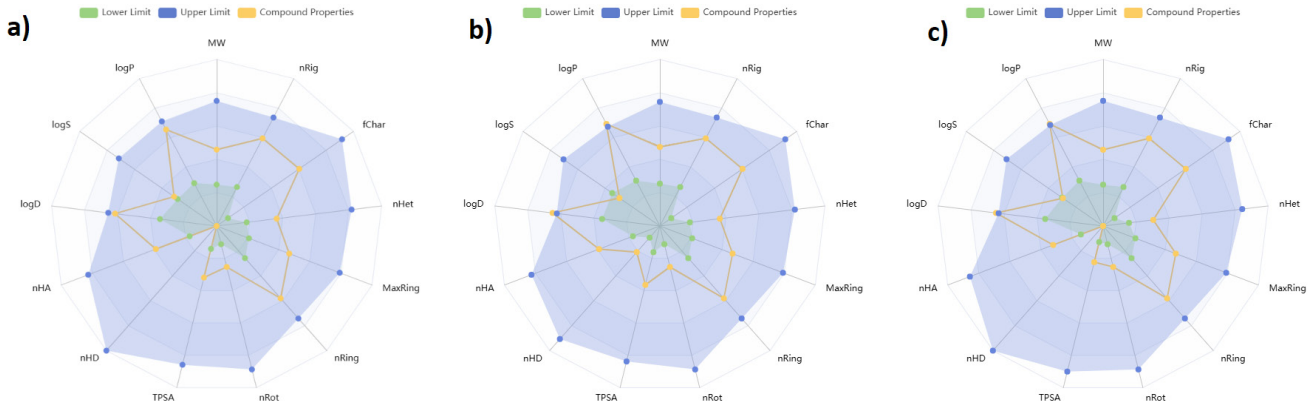

Figure 2. A radar-plot comparison of the predicted physicochemical profiles of thiazolo[3,2-*b*]triazol-7-ium cations **1**–**3** synthesized. Each panel illustrates the compound-specific descriptor values (orange) relative to the established lower (green) and upper (blue) thresholds associated with drug-likeness and acceptable oral bioavailability ranges. **(a)** Compound **1**. **(b)** Compound **2**. **(c)** Compound **3**.

Table 2. Physicochemical and absorption descriptors for compounds **1**–**3**

Descriptor	Compound			Comments
	1	**2**	**3**	
Molecular weight (MW, Da)	309.12	324.12	308.12	all below 500 Da, fulfilling the Lipinski's mass criterion
H-bond donors/acceptors (nHD/nHA)	0 / 4	1 / 4	0 / 3	introducing a phenolic OH in **2** increases the donor count and TPSA; the hydrogen-bond acceptor count includes hetero atoms of the fused thiazolotriazolium core (notably the N1 atom of the triazolium ring)
Topological polar surface area (TPSA, Å^2)	34.59	41.93	21.7	TPSA correlates with polarity; **2** is most polar due to the hydroxyl group
No rotatable bonds / rings / hetero atoms	2 / 4 / 5	2 / 4 / 5	2 / 4 / 4	a similar core rigidity across the series
Fraction of sp^3 carbons (Fsp3)	0.235	0.222	0.222	all highly aromatic cations (low Fsp3)
Predicted solubility logS	-3.73	-4.67	-4.07	negative values imply low aqueous solubility; **2** is least soluble
Predicted lipophilicity log*P*	2.61	3.15	3.06	**2** and **3** are more hydrophobic; **1** is more balanced
Caco-2 permeability (log cm s^{-1})	-5.19	-5.43	-5.02	values < −5 indicate poor intestinal permeability for all compounds
MDCK cell permeability (log cm s^{-1})	-4.53	-4.81	-4.63	consistent with the limited passive diffusion
Predicted human intestinal absorption (HIA)	≈ 0	≈ 0	≈ 0	extremely low (<10−5), reflecting the permanent cationic charge
Blood–brain barrier (BBB) permeability	0.114	0.006	0.181	probabilities < 0,5 indicate a negligible CNS penetration; only **3** shows a slightly higher score, but remains low
P-gp inhibition / substrate	inhibitor ≈1; substrate ≪1	inhibitor ≈1; substrate ≈0.01	inhibitor ≈1; substrate ≈0.0046	all three strongly inhibit P-gp while being poor substrates; this could the increase intracellular accumulation, but may cause drug–drug interactions
BCRP / BSEP	moderate BCRP (0.51–0.62) and strong BSEP inhibition (≈1) for all	similar for all	potential for the biliary transport inhibition	

compound **1**. All three cations exhibit very low predicted Caco-2 and MDCK permeabilities and negligible human intestinal absorption probabilities, consistent with their permanent positive charge and high polarity. The blood–brain barrier penetration is predicted to be minimal.

Table 3 shows that the compounds are predicted to have moderate volumes of distribution and strong plasma protein binding (> 90 %). Compound **1** has the highest unbound fraction (≈ 8 %), suggesting greater availability for the target engagement. Predicted elimination half-lives are short (< 0.5 h), implying rapid clearance although this may be offset by a high protein binding and potential transporter interactions. Bioconcentration factors are modest (≈ 2–3), indicating the limited environmental persistence.

Cations **1–3** differ in their predicted cytochrome P450 inhibition profiles. Compound **1** shows a strong inhibition of CYP2C19 and CYP2B6 and a moderate inhibition of CYP1A2, 2C9, 2D6, and 3A4, raising the possibility of drug–drug interactions. Compound **2** retains the strong CYP2C19 inhibition, but exhibits low probabilities of inhibiting other isoforms. Compound **3** shows an intermediate behavior, with the modest inhibition of CYP2B6 and CYP2C9 and the low inhibition of CYP1A2 and CYP2D6. None of the compounds are predicted to be CYP substrates.

ADMETlab predicts moderate to high probabilities of mutagenicity, carcinogenicity, drug-induced liver injury, and genotoxicity for all three compounds. Probabilities for nephrotoxicity, neurotoxicity, and hERG inhibition fall in the low to moderate range, suggesting some cardiotoxic and neurological risks. Skin sensitization probabilities are high. Among the three derivatives, compound **2** generally shows slightly lower toxicity scores.

The predicted ADMET profiles underscore both advantages and limitations of this scaffold. On the positive side, the cations satisfy fundamental drug-likeness criteria and exhibit a moderate lipophilicity, which can support the passive membrane diffusion. However, their predicted oral bioavailability is extremely low due to the poor permeability and permanent cationic charge, suggesting that the parenteral administration or prodrug strategies may be necessary. Compound **1** combines relatively better solubility with a higher risk of CYP-mediated interactions and toxicity; compound **2** has a lower solubility, but slightly reduced toxicity; compound **3** is the most hydrophobic and strongly protein-bound. Future optimization should therefore focus on enhancing the permeability and reducing the enzyme inhibition and toxicity while maintaining the beneficial aspects of the scaffold.

Molecular docking study

Taking into account the pronounced antifungal activity of compounds **1** and **2** against *Candida albicans* (**Table 1**), the molecular docking studies were primarily designed to investigate lanosterol 14-α-demethylase (CYP51, PDB ID: 5V5Z), a key enzyme in the ergosterol biosynthesis and a well-established molecular target of clinically used azole antifungals. The inhibition of CYP51 provides a direct and biologically plausible explanation for the antifungal effects of the thiazolotriazolium salts observed. The corresponding docking results and binding energy trends are summarized in **Table 4**.

For comparative and exploratory purposes only, docking calculations were additionally performed against two representative bacterial enzymes – MurB (PDB ID: 1MBT), involved in the bacterial cell wall biosynthesis, and DNA gyrase B (PDB ID: 4URO), a key enzyme in the DNA replication. These targets were selected as well-characterized, druggable antibacterial models supported by high-resolution crystal structures, allowing a preliminary assessment of potential antibacterial binding modes.

The docking against CYP51 revealed favorable binding affinities for compounds **2** and **3** (−8.6 kcal mol^{-1}), which moderately exceeded that of compound **1** (−8.0 kcal mol^{-1}). AutoDock Vina generated a single dominant binding pose for each

Table 3. Distribution, metabolism, and excretion for compounds **1–3**

Descriptor	Compound			Comments
	1	**2**	**3**	
Volume of distribution logVd	0.065	0.236	0.226	moderate volumes (0.1–0.3 L kg^{-1}) expected; **2** and **3** distribute slightly more than **1**
Fraction unbound (Fu, %)	8.16	4.15	1.54	compound **1** has the highest free fraction; **3** is almost completely protein-bound
Plasma protein binding (PPB, %)	90.2	94.9	98.1	all bind strongly to plasma proteins, particularly **3**
Elimination half-life (t1/2, h)	0.38	0.47	0.36	short predicted half-lives (<1 h) suggest rapid clearance
Bioconcentration factor (BCF)	2.18	2.12	2.85	slightly higher for **3**, but all are moderate

ISSN 2308-8303 (Print) / 2518-1548 (Online)

Table 4. The binding energies for compounds **1**–**3** with MurB (1MBT), DNA gyrase B (4URO), lanosterol 14-α-demethylase (5V5Z)

Protein (PDB ID)	Compound **1** (kcal mol^{-1})	Compound **2** (kcal mol^{-1})	Compound **3** (kcal mol^{-1})	Trend
Lanosterol 14-α-demethylase (5V5Z)	−8.0	−8.6	−8.6	2 ≈ 3 > 1
MurB (1MBT)	−8.9 (top pose)	−9.5 (strongest)	−9.3	2 > 3 > 1
DNA gyrase B (4URO)	−5.3	−5.7 (best)	−5.4	2 > 3 ≈ 1

ligand, suggesting a well-defined interaction mode within the enzyme active site.

All three compounds positioned their aromatic thiazolotriazolium core within a hydrophobic region of the CYP51 binding pocket. Compound **2** (3-hydroxyphenyl) adopted a particularly favorable orientation, in which the phenolic OH group formed a π-donor hydrogen bond / π-sulfur interaction with CYS470 (3.65 Å), accompanied by stabilizing π-alkyl interactions with ILE131 and ILE304 (**Figure 3**). This interaction pattern provides a clear structural rationale for the strong antifungal activity of compound **2** observed experimentally.

Compound **3** (phenyl) achieved a comparable binding energy through π–π stacking with TYR118 (≈ 3.80 Å) and hydrophobic contacts with CYS470 and ILE379, but lacked specific hydrogen-bonding interactions. In contrast, compound **1** (4-pyridyl) displayed a weaker binding, likely due to less optimal accommodation of the pyridyl substituent within the CYP51 pocket and the absence of strong directional hydrogen bonds.

The docking results against lanosterol 14-α-demethylase are fully consistent with the antifungal MIC data, supporting the CYP51 inhibition as a plausible molecular mechanism underlying the activity of compounds **1** and **2**, with the hydroxyl-substituted aromatic group in compound **2** conferring an additional binding advantage.

The complete interaction profiles and key contact distances for all protein–ligand complexes are summarized in **Table 5**.

The docking against MurB (PDB ID: 1MBT) yielded lower (more negative) binding energies than those obtained for DNA gyrase B. While compound **2** showed the strongest MurB affinity (−9.5 kcal mol^{-1}), this target did not directly explain the antifungal activity. Therefore, MurB is not considered the primary biological target in the present study.

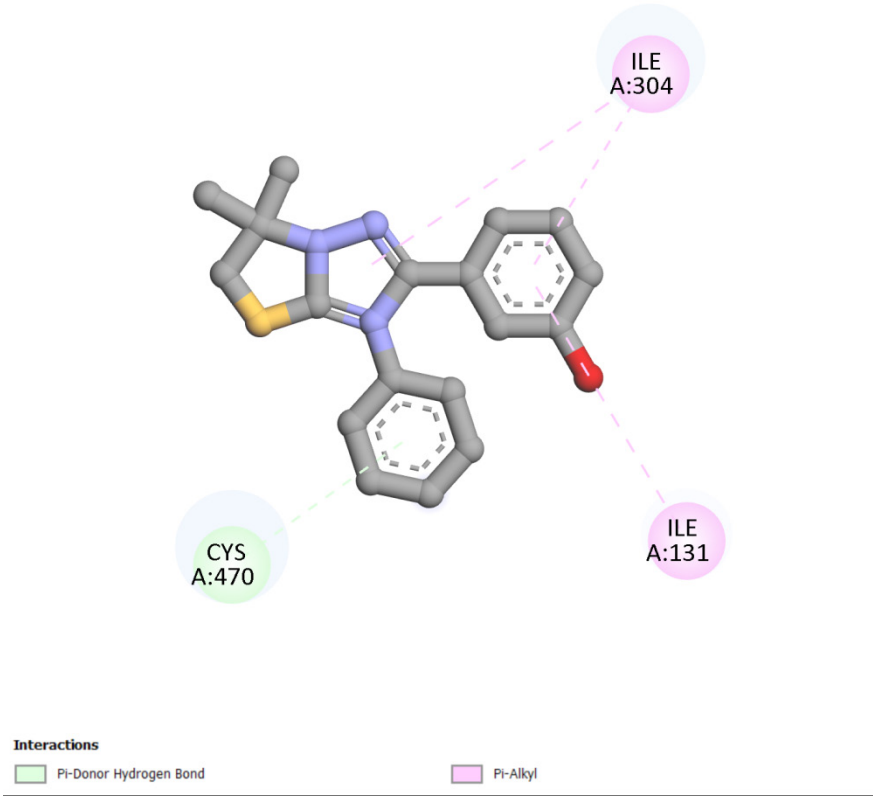

Figure 3. The predicted binding pose of compound **2** within the CYP51 active site (PDB ID: 5V5Z)

Table 5. The predicted protein–ligand interaction profiles of thiazolo[3,2-*b*]triazol-7-ium cations **1–3** with the key antimicrobial targets

Protein (PDB ID)	Compound	Key Interaction Type(s)	Interacting Residues (Protein)	Key Distances (A˚)
MurB (1MBT)	**1**	Conventional H-Bond, π-Alkyl	GLY47, VAL52, ILE119, ILE45, ILE173	H-Bond: 2.66
	2	2 Conventional H-Bonds, π-Cation, π-Alkyl	ASN65, ILE173, ARG327, ILE119, LEU46, ILE45	H-Bonds: 2.54, 2.52
	3	Conventional H-Bond, π-Alkyl	GLY47, VAL52, ILE45, ILE173, ILE119	H-Bond: 2.70
DNA Gyrase B (4URO)	**1**	π-Alkyl, Alkyl	LYS170	π-Alkyl: 4.14, 4.56
	2	π-Alkyl, Alkyl	LYS170	π-Alkyl: 4.15, 4.51
	3	Amide-π Stacked, π-Alkyl	LYS207, GLY208, ILE209	Amide-π: 3.94
Lanosterol 14-α-demethylase (5V5Z)	**1**	π-π Stacked, π-Alkyl, Alkyl	TYR118, CYS470, ILE379	π-π: 3.80
	2	π-Donor H-Bond/π-Sulfur, π-Alkyl	CYS470, ILE131, ILE304	H-Bond/π-Sulfur: 3.65
	3	π-π Stacked, π-Alkyl, Alkyl	TYR118, CYS470, ILE379	π-π: 3.80

All compounds exhibited poor binding to DNA gyrase B (−5.7 to −5.3 kcal mol^{-1}), with shallow, unstable binding modes and large RMSD values, indicating that the DNA gyrase inhibition was unlikely to contribute significantly to the biological effects observed.

The molecular docking results highlight lanosterol 14-α-demethylase (CYP51) as the most relevant molecular target for explaining the antifungal activity of thiazolotriazolium salts **1–3**. The favorable binding affinities and well-defined interaction patterns observed for compounds **2** and **3**, particularly the additional stabilizing interactions enabled by the phenolic OH group in compound **2**, are consistent with the experimentally determined antifungal MIC values.

■ Experimental part

General Information

All commercially available reagents and solvents were obtained from standard vendors and used without further purification unless otherwise stated. The starting methallyl thioethers were prepared according to the previously reported procedures [37]. ^{1}H NMR spectra were recorded using a Varian Mercury-400 instrument. Tetramethylsilane and deuterated dimethylsulfoxide were utilized in the NMR study as a standard and solvent, respectively. The elemental composition was determined with an Elementar Vario MICRO cube. Compounds **4, 5, 6** were previously reported (**4** – the sample **2a** [36]; **5** – the sample **2b** [36]; **6** – the sample **2d** [36]).

The General Procedure for the Synthesis of Compounds 1–3

The synthesis of thiazolo[3,2-*b*][1,2,4]triazol-7-ium hexabromotellurates was carried out *via* the electrophilic heterocyclization induced by tellurium(IV) species generated *in situ*. The mixture of 0.079 g of tellurium dioxide (TeO_2) in 1 mL acetonitrile, and 1 mL 48% hydrobromic acid (HBr) was stirred for 0.5 h until the formation of the H_2TeBr_6 complex. The corresponding methallyl thioether precursor (0.5 mmol) in 5 mL acetonitrile was subsequently added to the reaction mixture. The reaction mixture was heated for 1 h at 80–100 °C. Upon completion, the resulting orange colored precipitate was filtered, washed with a small amount of acetonitrile and ether, and dried to give the target hexabromotellurate salts **1–3** as crystalline solids.

6,6-Dimethyl-3-phenyl-2-(4-pyridyl)-5,6-dihydro-3H-[1,3]thiazolo[3,2-b][1,2,4]triazol-7-ium hexabromotellurate (**1**)

A bright orange-red solid. Yield – 0.39 g (64%) (55% [37]). M. p. 251–254 °C (decomp). Anal. Calcd for $C_{34}H_{34}Br_6N_8S_2Te$, %: C 33.31, H 2.80, N 9.14. Found, %: C 33.07, H 2.72, N 9.03. ^{1}H NMR (400 MHz, DMSO-d_6), δ, ppm: 1.78 (6H, s, $2CH_3$), 4.32 (2H, s, SCH_2), 7.54–7.65 (5H, m, Ph), 7.81 (2H, d, J = 4.5 Hz, Py-H), 8.56 (2H, d, J = 4.5 Hz, Py-H).

2-(3-Hydroxyphenyl)-6,6-dimethyl-3-phenyl-5,6-dihydro-3H-[1,3]thiazolo[3,2-b][1,2,4]triazol-7-ium hexabromotellurate (**2**)

A bright orange-red solid. Yield – 0.50 g (74%) (79% [37]). M. p. 262–263 °C (decomp). Anal. Calcd for $C_{36}H_{36}Br_6N_6O_2S_2Te$, %: C 34.43, H 2.89, N 6.69. Found, %: C 34.18, H 2.80, N 6.51. ^{1}H NMR (400 MHz, DMSO-d_6), δ, ppm: 1.76 (6H, s, $2CH_3$), 4.26 (2H, s, SCH_2), 6.80 (1H, d, J = 7.8 Hz, Ar-H), 6.85 (1H, s, Ar-H), 6.94 (1H, d, J = 8.0 Hz, Ar-H), 7.22 (1H, t, J = 8.0 Hz, Ar-H), 7.54–7.63 (5H, m, Ph).

6,6-Dimethyl-2,3-diphenyl-5,6-dihydro-3H-[1,3]thiazolo[3,2-b][1,2,4]triazol-7-ium hexabromotellurate (**3**)

A bright orange-red solid. Yield – 0.44 g (72%) (78% [37]). M. p. 256–258 °C (decomp). Anal. Calcd for $C_{36}H_{36}Br_6N_6S_2Te$, %: C 35.33, H 2.96,

ISSN 2308-8303 (Print) / 2518-1548 (Online)

N 6.87. Found, %: C 35.12, H 2.87, N 6.70. ^{1}H NMR (400 MHz, DMSO-d_6), δ, ppm: 1.76 (6H, s, 2CH_3), 4.24 (2H, s, SCH_2), 7.44–7.64 (10H, m, 2Ph).

Antimicrobial and Antifungal Activity Evaluation

The antimicrobial and antifungal activity of the compounds synthesized was evaluated in the Laboratory of the Research and Training Center for Molecular Microbiology and Immunology of Mucous Membranes, State Higher Educational Institution "Uzhhorod National University". Antibacterial and antifungal properties were determined by the serial dilution method to establish the minimum inhibitory concentration (MIC) and the minimum bactericidal concentration (MBC) values in accordance with CLSI M07 and EUCAST guidelines for *in vitro* antimicrobial testing [48].

For MIC and MBC testing, the contents of Eppendorf tubes with different dilutions of chemical compounds were re-inoculated onto solid nutrient media. The minimal concentration that completely inhibited the growth (no growth) was considered to be MBC. The minimal concentration that significantly inhibited the growth of microorganisms compared to the control was considered as MIC. Microbial test cultures included *Staphylococcus aureus*, *Candida albicans*, *Klebsiella pneumoniae*, *Escherichia coli*, and *Pseudomonas aeruginosa*. The strains of bacteria and fungi under research were clinical isolates collected from the parodontal pockets of patients with chronic generalized periodontitis who underwent treatment at the Uzhhorod University dental clinic. Microbial suspensions were prepared from 24-hour cultures on the appropriate media and adjusted to a 0.5 McFarland standard (≈ 1.5 × 10^8 CFU mL^{-1}). Each well of a sterile 96-well plate received 10 μL of the standardized microbial suspension and 100 μL of the compound solution prepared in the sterile broth. Control groups were: (1) the microbial growth control – inoculated medium without the compound (to verify viability); (2) the compound sterility control – the compound solution without the inoculum (to exclude contamination); (3) the solvent control – the medium with the solvent only in the working concentration (to eliminate the solvent antimicrobial effect). Plates were incubated at 37 °C for 24 h, followed by titration via serial 2-fold dilutions and reseeding onto selective agar media (MPA, Sabouraud, Endo, MRS, Enterococcus agar). After 24–48 h of incubation, the colony growth or the absence was visually assessed to determine MIC and MBC. All procedures were conducted under sterile conditions; sterility of the preparations was confirmed bacteriologically by plating 10 μL aliquots on the meat-peptone agar. Antimicrobial susceptibility tests with reference drugs were performed for all clinical isolates studied using the disc-diffusion Kirby-Bauer method [49] and the serial 2-fold dilution method to determine MIC and MBC. To compare the activity of the compounds studied with that of antibiotics, the latter were diluted to the same concentration range (250–15.625 μg mL^{-1}). Data about the susceptibility of the bacteria under research are given in **Table 6**.

Computational Methodology

ADMET Prediction

The pharmacokinetic properties and toxicity profiles of the compounds were predicted using the ADMETlab 3.0 web server [42]. Key parameters calculated included physicochemical descriptors (MW, TPSA, log*P*, logS), absorption (Caco-2 permeability, HIA), distribution (PPB, BBB penetration), metabolism (CYP450 inhibition), and toxicity endpoints (AMET test, hepatotoxicity).

Molecular Docking

Docking runs were performed with AutoDock Vina [50, 51] to evaluate how cations **1–3** interacted with MurB (UDP-*N*-acetylenolpyruvoylglucosamine reductase, PDB ID 1MBT), DNA gyrase B (ATPase subunit of bacterial topoisomerase, PDB ID 4URO), and lanosterol 14-α-demethylase (CYP51) from *Candida albicans* (PDB ID 5V5Z). Protein coordinates were downloaded from the Protein Data Bank and prepared using AutoDock Tools: water molecules

Table 6. Antimicrobial and antifungal susceptibility tests with reference drugs

Reference drug	MIC/MBC (μg mL^{-1})				
	C. albicans	*S. aureus*	*K. pneumoniae*	*E. coli*	*P. aeruginosa*
Fluconazol	<15.625	ND[a]	ND[a]	ND[a]	ND[a]
Levofloxacin	ND[a]	<15.625	<15.625	<15.625	<15.625
Lincomycin	ND[a]	<15.625	250 / >250	>250	>250
Amikacin	ND[a]	<15.625	31.25 / 62.5	31.25 / 31.25	62.5 / 62.5
Gentamicin	ND[a]	<15.625	61.5 / 125	31.25 / 125	125 / 250

Note: [a] ND – not determined. As the dilution range was 250-15.625 μg mL^{-1}, in some cases the MIC and MBC values were below (<15.625 μg mL^{-1}) or above (>250 μg mL^{-1}) the concentration range studied.

and any non-essential ligands were removed, polar hydrogens were added, and Gasteiger charges were assigned; essential cofactors were preserved. Each ligand was geometry-optimized and converted to *.pdbqt format before being docked individually into each receptor's active site. For MurB, the search grid was centered at X = 11.056, Y = 38.244 and Z = 18.464 with dimensions of 60 × 60 × 60 Å; DNA gyrase B used a center at X = 24.675, Y = –9.190 and Z = –26.488 with the same box size; the CYP51 enzyme employed a grid centered at X = –41.072, Y = –13.759 and Z = 25.140, and 60 Å per side. AutoDock Vina reports affinities in kcal mol^{-1}, with more negative scores indicating tighter predicted binding [52]; for each compound, the top-ranked pose was used for the subsequent analysis. The resulting complexes were visualized and their interactions examined in the BIOVIA Discovery Studio Visualizer [53].

Conclusion

An effective synthesis of a novel series of thiazolo[3,2-*b*]triazol-7-ium hexabromotellurates **1–3** has been successfully carried out. We have demonstrated the successful cyclization using the TeO_2/HBr electrophilic system under optimized reaction conditions. A systematic study of the structure–activity relationships has shown that substitutions in position 5 of the core heterocycle profoundly affect the antimicrobial efficacy – the introduction of a polar substituent with π-conjugated functionality in position 2 of the target [1,3]thiazolo[3,2-*b*][1,2,4]triazol-7-ium salts can improve the antimicrobial properties of the latter.

The high antifungal potency against *C. albicans* (MIC 15.625 μg mL^{-1}) was consistently observed for the derivatives containing polar groups, namely the 4-pyridyl (compound **1**) and the 3-hydroxyphenyl (compound **2**) derivatives. Crucially, the 4-pyridyl derivative (compound **1**) demonstrated the selective and potent activity against the Gram-negative bacterium *E. coli* (MIC 31.25 μg mL^{-1}), positioning it as the most promising lead candidate in this series.

Molecular docking studies support lanosterol 14-α-demethylase (CYP51) as a plausible molecular target underlying the antifungal activity observed. The enhanced binding affinities of compounds **2** and **3** are rationalized by favorable noncovalent interactions within the CYP51 active site, with the phenolic OH group of compound **2** enabling additional stabilizing contacts, while weaker binding of compound **1** reflects less optimal accommodation of the pyridyl substituent. In contrast, the docking against bacterial targets suggests that DNA gyrase B is unlikely to represent the primary mode of action.

These findings validate the strategy of combining a highly cationic thiazolotriazolium scaffold with a metal-complexed anion ($TeBr_6^{-2}$) to generate potent antimicrobial agents with a tunable selectivity. Future studies will focus on the structural optimization of lead compound **1**, elucidation of its precise cellular mode of action, and evaluation against clinically relevant multidrug-resistant strains.

References

1. Murray, C. J. L.; Ikuta, K. S.; Sharara, O. A., et al. Global burden of bacterial antimicrobial resistance 1990–2021: a systematic analysis with forecasts to 2050. *The Lancet* **2024**, *404* (10459), 1199–1226. https://doi.org/10.1016/S0140-6736(24)01867-1.
2. Tacconelli, E.; Carrara, E.; Savoldi, A., et al. Discovery, research, and development of new antibiotics: the WHO priority list of antibiotic-resistant bacteria and tuberculosis. *Lancet Infect. Dis*. **2018**, *18* (3), 318–327. https://doi.org/10.1016/S1473-3099(17)30753-3.
3. Ventola, C. L. The antibiotic resistance crisis: Part 1: Causes and threats. *P & T* **2015**, *40* (4), 277–283.
4. Cella, E.; Giovanetti, M.; Benedetti, F.; Scarpa, F.; Johnston, C.; Borsetti, A.; Ceccarelli, G.; Azarian, T.; Zella, D.; Ciccozzi, M. Joining Forces against Antibiotic Resistance: The One Health Solution. *Pathogens* **2023**, *12*, 1074. https://doi.org/10.3390/pathogens12091074.
5. Gattu, R.; Ramesh, S.S.; Ramesh, S. Role of small molecules and nanoparticles in effective inhibition of microbial biofilms: A ray of hope in combating microbial resistance. *Microb. Pathog*. **2024**, *188*, 106543. https://doi.org/10.1016/j.micpath.2024.106543.
6. Jampilek, J. Heterocycles in Medicinal Chemistry. *Molecules* **2019**, *24* (21), 3839. https://doi.org/10.3390/molecules24213839.
7. Łowicki, D.; Przybylsk, P. Piperidine-containing drugs and recently studied analogs – biological activity, mechanism of action and synthetic cascade access to their scaffolds. *Eur. J. Med. Chem.* **2025**, *302* (1), 118213. https://doi.org/10.1016/j.ejmech.2025.118213.
8. Manhas, N.; Kumar, G.; Dhawan, S.; Makhanya, T.; Singh, P. A Systematic Review of Synthetic and Anticancer and Antimicrobial Activity of Quinazoline/Quinazolin-4-one Analogues. *ChemistryOpen*. **2025**, *14* (7), e202400439. https://doi.org/10.1002/open.202400439.
9. Sousa, M. H. O.; Silva, C. H. L.; Silveira, M. V.; Godoi, M. Recent progress in 1-thioflavones and 4-thioflavones: Synthesis, applications and prospects. *Phosphorus Sulfur Silicon Relat. Elem.* **2025**, 1–34. https://doi.org/10.1080/10426507.2025.2578201.
10. Khidre, R. E.; Borik, R. M.; Behalo, M. S.; Elkarim, I. A. G.; Esam, A. Synthetic Methods and Pharmacological Potentials of Isothiocyanate Derivatives. *Mini-Rev. Org. Chem.* **2025**, *22* (6), 638–652. https://doi.org/10.2174/0118756298328213240904051112.
11. La Monica, G.; Bono, A.; Alamia, F.; Lauria, A.; Martorana, A. Bioisosteric heterocyclic analogues of natural bioactive flavonoids by scaffold-hopping approaches: State-of-the-art and perspectives in medicinal chemistry. *Bioorg. Med. Chem.* **2024**, *109*, 117791. https://doi.org/10.1016/j.bmc.2024.117791.
12. Morlion, F.; Magdalenic, K.; Van Camp, J.; D'hooghe, M. Heterocycle-substituted 1,5-benzothiazepines: biological properties and structure–activity relationships. *Monatsh Chem*. **2024**, *155*, 535–549. https://doi.org/10.1007/s00706-024-03195-3.

ISSN 2308-8303 (Print) / 2518-1548 (Online)

13. Khamitova, K.; Berillo, D.; Lozynskyi, A.; Konechnyi, Y.; Mural, D.; Georgiyants, V.; Lesyk, R. Thiadiazole and thiazole derivatives as potential antimicrobial agents. *Mini-Rev. Med. Chem*. **2024**, *24* (5), 531–545. https://doi.org/10.2174/1389557523666230713115947.
14. Korol, N.; Molnar-Babilya, D.; Slivka, M.; Onysko, M. A brief review on heterocyclic compounds with promising antifungal activity against Candida species. *Org. Commun*. **2022**, *15* (4), 304–323. https://doi.org/10.25135/acg.oc.141.2210.2609.
15. Slivka, M. V.; Korol, N. I. Condensed pyridopyrimidines and pyridopyrazines containing a bridgehead nitrogen atom: synthesis, chemical properties and biological activity. *Curr. Org. Chem*. **2021**, *25* (12), 1429–1440. https://doi.org/10.2174/1385272825666210525154330.
16. Hryhoriv, H.; Kovalenko, S.M.; Georgiyants, M.; Sidorenko, L.; Georgiyants, V. A. Comprehensive Review on Chemical Synthesis and Chemotherapeutic Potential of 3-Heteroaryl Fluoroquinolone Hybrids. *Antibiotics* **2023**, *12* (3), 625. https://doi.org/10.3390/antibiotics12030625.
17. Swathykrishna, C. S.; Amrithanjali, G.; Shaji, G.; Kumar R. A. Antimicrobial Activity and Synthesis of Thiazole Derivatives: A Recent Update. *J. Chem. Rev*. **2023**, *5* (3), 221–240. https://doi.org/10.22034/JCR.2023.383674.1211.
18. Korol, N. I.; Slivka, M. V. Recent progress in the synthesis of thiazolo [3,2-*b*][1,2,4]triazoles (microreview). *Chem. Heterocycl. Compd*. **2017**, *53* (8), 852–854. https://doi.org/10.1007/s10593-017-2136-3.
19. Slivka, M. V.; Korol, N. I.; Fizer, M. M. Fused bicyclic 1,2,4-triazoles with one extra sulfur atom: Synthesis, properties, and biological activity. *J. Heterocycl. Chem.* **2020**, *57* (9), 3236–3254. https://doi.org/10.1002/jhet.4044.
20. Farveen, M. D., Kalagara, S., Balraju, E., Jaysree, B., Shaik, A., Alia, B. Discovery of novel Quinazoline based Thiazolotriazole hybrids as potential EGFR inhibitor: Synthesis, anticancer evaluation and in silico studies. *Chem. Biol. Lett.* **2025**, *12* (2), 1261–1261. https://doi.org/10.62110/sciencein.cbl.2025.v12.1261.
21. Rostom, S. A.; Badr, M. H.; Abd El Razik, H. A.; Ashour, H. M. Structure-based development of novel triazoles and related thiazolotriazoles as anticancer agents and Cdc25A/B phosphatase inhibitors. Synthesis, *in vitro* biological evaluation, molecular docking and *in silico* ADME-T studies. *Eur. J. Med. Chem*. **2017**, *139*, 263–279. https://doi.org/10.1016/j.ejmech.2017.07.053.
22. Barbuceanu, S. F.; Draghici, C.; Barbuceanu, F.; Bancescu, G.; Saramet, G. Design, synthesis, characterization and antimicrobial evaluation of some heterocyclic condensed systems with bridgehead Nitrogen from thiazolotriazole class. *Chem. Pharm. Bull.* **2015**, *63* (9), 694–700. https://doi.org/10.1248/cpb.c15-00379.
23. Almasirad, A.; Sani, P. S. V.; Mousavi, Z.; Fard, G. B.; Anvari, T.; Farhadi, M.; Vosooghi, M.; Azizian, H. Novel thiazolotriazolone derivatives: design, synthesis, in silico investigation, analgesic and anti-inflammatory activity. *ChemistrySelect*. **2022**, *7* (28), e202103228. https://doi.org/10.1002/slct.202103228.
24. Slivka, M.; Onysko, M. The use of electrophilic cyclization for the preparation of condensed heterocycles. *Synthesis*. **2021**, *53* (19), 3497–3512. https://doi.org/10.1055/s-0040-1706036.
25. Kut, D.; Kut, M.; Komarovska-Porokhnyavets; O., Kurka; M., Onysko, M.; Lubenets, V. Antimicrobial activity of halogen-and chalcogen-functionalized thiazoloquinazolines. *Lett. Drug Des. Discovery*. **2024**, *21* (13), 2490–2496. https://doi.org/10.2174/1570180820666230726160348.
26. Pantyo, V. V.; Haleha, O. V.; Kut, D. Z.; Kut, M. M.; Onysko, M. Y.; Danko, E. M.; Koval G.M.; Pantyo V.I.; Haza K.V.; Bulyna, T. B. The effect of low-intensity laser radiation on the sensitivity of *Staphylococcus aureus* to some halogen-containing azaheterocycles. *Regulatory Mechanisms in Biosystems*. **2024**, *15* (2), 230–234. https://doi.org/10.15421/022434.
27. Kut, M. M.; Onysko, M. Y. Aryltellurium trihalides in the synthesis of heterocyclic compounds (microreview). *Chem. Heterocycl. Compd.* **2020**, *56* (5), 503–505. https://doi.org/10.1007/s10593-020-02688-3.
28. Sabti, A.B.; Al-Fregi, A.A.; Yousif, M.Y. Synthesis and antimicrobial evaluation of some new organic tellurium compounds based on pyrazole derivatives. *Molecules* **2020**, *25* (15), 3439–3456. http://dx.doi.org/10.3390/molecules25153439.
29. Al-Fregi, A.A.; Al-Salami, B.K.; Al-Khazragie, Z.K.; Al-Rubaie, A.Z. Synthesis, characterization and antibacterial studies of some new tellurated azo compounds. *Phosphorus Sulfur Silicon Relat. Elem.* **2019**, *194*, 33–38. http://dx.doi.org/10.1080/10426507.2018.1470179.
30. Halpert, G.; Halperin Sheinfeld, M.; Monteran, L.; Sharif, K.; Volkov, A.; Nadler, R.; Schlesinger, A.; Barshak, I.; Kalechman, Y.; Blank, M.; Shoenfeld, Y.; Amital, H. The tellurium-based immunomodulator, AS101 ameliorates adjuvant-induced arthritis in rats. *Clin. Exp. Immunol.* **2021**, *203*(3), 375–384. http://dx.doi.org/10.1111/cei.13553.
31. Cabrera, N.; Mora, J.R.; Márquez, E.; Flores-Morales, V.; Calle, L.; Cortés, E. QSAR and molecular docking modelling of anti-leishmanial activities of organic selenium and tellurium compounds. *SAR QSAR Environ. Res.* **2021**, *32*(1), 29–50. http://dx.doi.org/10.1080/1062936X.2020.1848914.
32. Ba, L. A.; Döring, M.; Jamier, V.; Jacob, C. Tellurium: An element with great biological potency and potential. *Org. Biomol. Chem.* **2010**, *8* (19), 4203–4216. https://doi.org/10.1039/C0OB00086H.
33. Vávrová, S.; Struhárňanská, E.; Turňa, J.; Stuchlík, S. Tellurium: A Rare Element with Influence on Prokaryotic and Eukaryotic Biological Systems. *Int. J. Mol. Sci.* **2021**, *22* (11), 5924. https://doi.org/10.3390/ijms22115924.
34. Slivka, M.; Fizer, M.; Mariychuk, R.; Ostafin, M.; Moyzesh, O.; Koval, G.; Holovko-Kamoshenkova, O.; Rusyn, I.; Lendel, V. Synthesis and Antimicrobial Activity of Functional Derivatives of thiazolo [2,3-*c*][1,2,4] triazoles. *Lett. Drug Des. Discovery* **2022**, *19* (9), 791–799. https://doi.org/10.2174/1570180819666220110145659.
35. Slivka, M.; Korol, N.; Pantyo, V.; Baumer, V.; Lendel, V. Regio-and stereoselective synthesis of [1,3]thiazolo[3,2-*b*][1,2,4]triazol-7-ium salts via electrophilic heterocyclization of 3-*S*-propargylthio-4*H*-1,2,4-triazoles and their antimicrobial activity. *Heterocycl. Commun.* **2017**, *23* (2), 109–113. https://doi.org/10.1515/hc-2016-0233.
36. Slivka, M.; Sharga, B.; Pylypiv, D.; Aleksyk, H.; Korol, N.; Fizer, M.; Fedurcya, O.; Pshenychnyi, O.; Mariychuk, R. [1,3]Thiazolo[3,2-*b*]-[1,2,4]triazolium Salts as Effective Antimicrobial Agents: Synthesis, Biological Activity Evaluation, and Molecular Docking Studies. *Int. J. Mol. Sci.* **2025**, *26* (14), 6845. https://doi.org/10.3390/ijms26146845.
37. Fizer, M., Slivka, M., Baumer, V. (2021). Efficient synthesis of substituted [1,3] thiazolo [3,2-b][1,2,4]triazol-7-ium hexabromotellurates. *J. Organomet. Chem.* **2021**, *952*, 122044. https://doi.org/10.1016/j.jorganchem.2021.122044.
38. Biot, N.; Romito, D.; Bonifazi, D. Substituent-Controlled Tailoring of Chalcogen-Bonded Supramolecular Nanoribbons in the Solid State. *Crystal Growth & Design*. **2021**, *21* (1), 536–543. https://doi.org/10.1021/acs.cgd.0c01318.
39. Ungureanu, D.; Tiperciuc, B.; Nastasă, C.; Ionuț, I.; Marc, G.; Oniga, O.; Oniga, I. An Overview of the Structure–Activity Relationship in Novel Antimicrobial Thiazoles Clubbed with Various Heterocycles (2017–2023). *Pharmaceutics* **2024**, *16*, 89. https://doi.org/10.3390/pharmaceutics16010089.
40. Mohanty, P.; Jena, S.; Rout, L.; et al. Antibacterial Activity of Thiazole and Its Derivatives: A Review. *Biointerface Res. Appl. Chem.* **2021**, *11*, 2172–2187. https://doi.org/10.33263/BRIAC122.21712195.
41. Goyal, A.; Bhandari, M. Synthetic and therapeutic review of triazoles and hybrids. *Heterocycl. Commun.* **2024,** *30* (1), 20220174. https://doi.org/10.1515/hc-2022-0174.

42. Fu, L.; Shi, S.; Yi, J.; Wang, N.; He, Y.; Wu, Z.; Cao, D. ADMETlab 3.0: An Updated Comprehensive Online ADMET Prediction Platform. *Nucleic Acids Res.* **2024**, *52* (W1), W422–W431. https://doi.org/10.1093/nar/gkae236.
43. Xiong, G.; Wu, Z.; Yi, J.; Fu, L.; Yang, Z.; Hsieh, C.; Cao, D. ADMETlab 2.0: An Integrated Online Platform for Accurate and Comprehensive Predictions of ADMET Properties. *Nucleic Acids Res.* **2021**, *49* (W1), W5–W14. https://doi.org/10.1093/nar/gkab255.
44. Guan, L.; Yang, H.; Cai, Y.; Sun, L.; Di, P.; Li, W.; Liu, G.; Tang, Y. ADMET-score - a comprehensive scoring function for evaluation of chemical drug-likeness. *Medchemcomm* **2019**, *10* (1), 148–157. https://doi.org/10.1039/c8md00472b.
45. Dulsat, J.; Lopez, A.; Fuguet, E.; et al. Evaluation of Free Online ADMET Tools for Academic or Commercial Use. *Molecules* **2023**, *28* (2), 776. https://doi.org/10.3390/molecules28020776.
46. Klimoszek, D.; Ziecik, A.; Kowalska, J.; et al. Study of the Lipophilicity and ADMET Parameters of New Compounds. *Pharmaceuticals* **2024**, *17* (6), 725. https://doi.org/10.3390/ph17060725.
47. Yakobi, S.; Zuckerman, O.; Cohen, S.; et al. Molecular Docking and Structure-Activity Relationship of Novel Heterocyclic Scaffolds. *ChemistrySelect* **2024**, *9*, e202303341. https://doi.org/10.1002/slct.202303341.
48. European Committee on Antimicrobial Susceptibility Testing. EUCAST Reading Guide for Broth Microdilution. Version 5.0 (January 2024). https://www.eucast.org/fileadmin/eucast/pdf/MIC/Reading_guide_BMD_v_5.0_2024.pdf.
49. European Committee on Antimicrobial Susceptibility Testing. EUCAST Disk Diffusion Method for Antimicrobial Susceptibility Testing. Version 13.0 (January 2025). https://www.eucast.org/fileadmin/eucast/pdf/disk_test_documents/2025/Manual_v_13.0_EUCAST_Disk_Test_2025.pdf.
50. Ubaid, A.; Shakir, M.; Ali, A.; Khan, S.; Alrehaili, J.; Anwer, R.; Abid, M. Synthesis and SAR Studies on New 4-Aminoquinoline-Hydrazones and Isatin Hybrids. *Molecules* **2024**, *29* (23), 5777. https://doi.org/10.3390/molecules29235777.
51. Trott, O.; Olson, A. J. AutoDock Vina: Improving the Speed and Accuracy of Docking with a New Scoring Function, Efficient Optimization, and Multithreading. *J. Comput. Chem.* **2010**, *31* (2), 455–461. https://doi.org/10.1002/jcc.21334
52. Eberhardt, J.; Santos-Martins, D.; Tillack, A.F.; Forli, S. AutoDock Vina 1.2.0: New Docking Methods, Expanded Force Field, and Python Bindings. *J. Chem. Inf. Model.* **2021**. https://doi.org/10.1021/acs.jcim.1c00203
53. BIOVIA, Dassault Systèmes. *BIOVIA Discovery Studio Visualizer*; Dassault Systèmes: San Diego, CA, **2019**.

Information about the authors:
Nataliya I. Korol, Candidate of Chemistry, Associate Professor of the Organic Chemistry Department, Uzhhorod National University; https://orcid.org/0000-0001-7155-1676.
Valeriy V. Pantyo, Candidate of Biology, Associate Professor of the Microbiology, Virology, Epidemiology, with the Course Infectious Department, Uzhhorod National University; https://orcid.org/0000-0002-0207-3372.
Victoriia O. Bestritska, Engineer of the Organic Chemistry Department, Uzhhorod National University; https://orcid.org/0009-0009-2437-8773.
Kamila A. Avdeeva, Master's Degree Student of the Pharmaceutical Disciplines Department, Uzhhorod National University.
Dzhosiya I. Molnar-Babilya, Candidate of Chemistry, Associate Professor of the Hotel and Restaurant Business Department, Ferenc Rákóczi II Transcarpathian Hungarian Institute; Associate Professor of the Department of Hotel and Restaurant Business, Mukachevo State University; https://orcid.org/0000-0003-1063-013X.
Maksym M. Fizer, Candidate of Chemistry, Associate Professor, Research Assistant Professor of the Department of Chemistry, University of Nevada Reno; https://orcid.org/0000-0001-6583-3159.
Mykhailo V. Slivka (*corresponding author*), Dr.Sci. in Chemistry, Professor, Professor of the Organic Chemistry Department, Uzhhorod National University; https://orcid.org/0000-0003-4788-0511; e-mail for correspondence: mikhailo.slivka@uzhnu.edu.ua.

ISSN 2308-8303 (Print) / 2518-1548 (Online)